

B. Rubinsky  
A. Shitzer

Faculty of Mechanical Engineering,  
Technion-Israel Institute of Technology,  
Haifa, Israel

# Analysis of a Stefan-Like Problem in a Biological Tissue Around a Cryosurgical Probe

*Analysis of a Stefan-like problem in the in vivo freezing of a biological tissue is presented in cartesian coordinates. The analysis allows the inclusion of blood perfusion, metabolic heat and tissue heat capacity. Solutions are obtained for the temperature distributions in the frozen and unfrozen regions at different times. A constant freezing rate, in accordance with the optimal tissue destruction rate, is assumed. Results indicate the importance of the blood perfusion factor in the problem and allow the prediction of probe temperature and heat flux variations for optimal results in tissue destruction.*

## Introduction

Cryosurgery deals with the controlled destruction of biological cells due to deep freezing and thawing. Freezing of cells involves the removal of pure water from both the intercellular and the extracellular solutions. The water freezes, as the temperature is dropped, into biologically inert foreign ice crystal. The rates of ice crystal nucleation and growth are both temperature and vapor pressure dependent. Evidence in the literature indicates that the rate of cooling at the frozen-unfrozen tissue interface is of prime importance in determining the percentage of surviving cells [1].<sup>1</sup> There is also evidence that the rate of thawing influences the destruction rate of the cells too, with the least number of cells surviving a slow rate of thawing immediately following rapid freezing [1-4]. According to Farrant only a small number of cells are destroyed by low temperatures alone [1]. As discussed in the literature [2-4], at slow cooling rates formation of ice crystals in the extracellular solutions will occur first. These crystals will cause the shrinkage of the cell. At high cooling rates, however, the intercellular water will freeze before shrinkage will have occurred.

Two mechanisms are commonly assumed to be involved in the destruction of biological cells during the freezing and thawing processes. "At a slow cooling rate it is presumed that damage is linked to the consequences of a raised concentration of extracel-

lular solutes interacting on the shrunken cell. As damage is due to the uptake of extracellular solutes through a leaky membrane, then as the cooling rate becomes faster there will be less time for this (phenomenon) to take place and damage will be reduced at higher cooling rates" [1]. At higher cooling rates, however, damage is correlated with the formation of intercellular ice before shrinkage occurs thus reducing the number of surviving cells [5, 6].

It should be noted that each cell type was found to possess a different survival curve, i.e., number of surviving cells versus cooling rate. Thus, a certain cooling rate may not cause formation of intercellular ice in one cell type whereas the opposite might hold for another cell type. An example of this phenomenon might be given by observing mouse embryos and red blood cells. Cooling rates larger than 2°C/min will cause intercellular ice to form in mouse embryos while only at 850°C/min will the same occur in red blood cells. Thus, a selective destruction of certain cell types in a tissue might be achieved should their particular survival curves be known.

Cryosurgery has been applied for a number of years to the destruction of malignant and other tissues. Cryosurgical devices come in various shapes and sizes as reviewed by Barron [7]. As the probe is introduced into the tissue and the flow of the cryofluid is initiated, a frozen front starts to form. A physician employing this technique is faced with two basic difficulties: one is the extent to which the frozen front has penetrated, and the second is the possible percentage of destroyed cells to be expected in the tissue [1].

Attempts in the literature were directed at obtaining the location of the frozen front by analytical methods. In 1968, Barron published a paper dealing with heat transfer problems in cryosurgery. Assuming a constant heat flux at the probe surface, he obtained solutions for the ice sphere radius and probe-tip temperature variations [8]. Barron did not consider the effects of either

<sup>1</sup> Numbers in brackets designate References at end of paper.

Contributed by the Heat Transfer Division for publication in the JOURNAL OF HEAT TRANSFER. Manuscript received by the Heat Transfer Division September 25, 1975. Paper No. 76-HT-PP.

blood perfusion or heat generation in the tissue. Assuming a constant probe-tip temperature Trezek and Cooper presented in spherical coordinates a numerical solution which was quite time consuming [9]. In a subsequent paper by the same authors an approximate analytical solution to the rate of growth of the frozen front for the same conditions was presented [10]. In this second work the authors assumed that the heat capacity of both the frozen and unfrozen regions are negligible compared to the latent heat of fusion. This assumption permits the determination of a quasi-steady temperature field. Recently, Warren and co-workers presented an approximate integral technique solution to this problem in cartesian coordinates [11]. They assumed the temperature of the cryofluid to be constant with the probe surface temperature varying until it reaches that of the cryofluid. The temperature distribution in the tissue was taken as a second-degree polynomial while neglecting the metabolic heat rate, and with the heat capacity also neglected relative to the latent heat of fusion.

The purpose of the present paper is to obtain an analytical solution to the problem of freezing of biological tissues taking into account heat capacity, blood perfusion, and metabolic heat rate so that a large enough cooling rate at the frozen-unfrozen tissue interface be produced. As noted previously, the achievement of this minimal cooling rate at the freezing front is of utmost importance where maximum destruction rate is desired. The analysis is presented in cartesian coordinates for simplicity and should, thus, be regarded as a first approximation to the solution of the problem.

### Analysis

Heat transfer in the living tissue is assumed to be governed by the bio-heat equation [12]. In the frozen region diffusion of heat is described by the heat equation. For both regions the physical and thermophysical properties are assumed homogeneous and constant. The entire tissue is assumed at a constant temperature prior to the initiation of the flow of the cryofluid in the probe. This assumption was shown to be valid at the deeper layers of the tissue [13] and might further be assumed as a good approximation for small volumes of the tissue.

Difference between deep body temperature and blood stream temperature at steady state is assumed constant. The magnitude of this difference is directly proportional to the total metabolic rate and inversely proportional to the average blood perfusion rate [9].

As for blood perfusion and volumetric metabolic rates, two assumptions were tried. One was that both these quantities remain constant throughout the cooling period and then drop to zero when freezing commences. The constancy of blood perfusion rate prior to freezing was observed by Rothenberg [14]. He claims that due to the high rate of cooling applied during cryosurgery, the blood vessels do not have sufficient time to contract, thus, blood continues to flow until it freezes as a bulk. This assumption is also in accordance with Walder [15] and Chato [16]. The second assumption

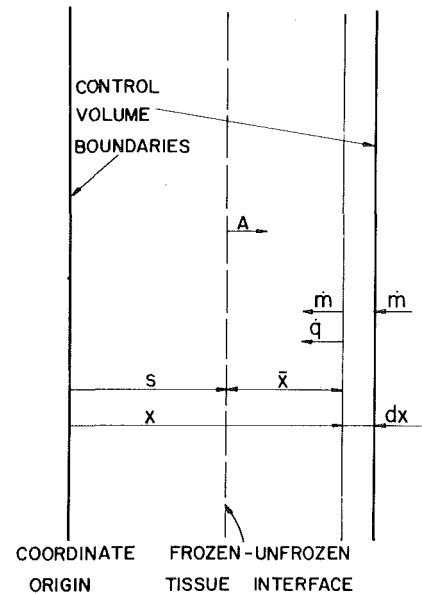


Fig. 1 Schematic drawing of control volume used in the analysis

was identical for the blood perfusion rate while the volumetric metabolic rate was assumed to drop linearly to zero with tissue temperature. This linear variation of the metabolic rate could not be supported by the literature and was assumed for the purpose of studying its influence on tissue temperature. It turned out that this second assumption complicated the analysis slightly but did not change the results significantly. Therefore, the first assumption is used in the analysis.

The problem is divided into two time domains:  $t < t_0$  and  $t > t_0$  where  $t_0$  denotes the time of formation of the first ice crystals. In the first time interval, lowering of tissue temperature to the freezing level takes place. In the second, freezing of the tissue adjacent to the probe occurs with the advancement of the frozen front. At the beginning of the second time interval, temperature distribution immediately preceding formation of the first ice crystals is assumed to be compatible with that obtained by the analysis of the freezing region. This could be obtained by varying the temperature of the probe in a certain manner which will be described later.

The analysis of the freezing region is performed according to the technique of solution of the ablation problem [17]. Temperature distributions in the frozen region are based on solutions to the inverse Stefan problem [18].

The control volume for which the analysis is performed is shown in Fig. 1. In this figure the location of the frozen front is indicated

### Nomenclature

$A$  = frozen-unfrozen interface velocity

$B$  = imaginary temperature in equation (13); defined by equation (14)

$c_b$  = specific heat of blood

$c_p$  = specific heat of tissue

$h$  = modified Peclet number, defined by equation (18)

$H$  = frozen-unfrozen interface cooling rate

$k$  = thermal conductivity of unfrozen tissue

$k_f$  = thermal conductivity of frozen tissue

$L$  = latent heat of fusion of water

$\dot{m}$  = imaginary mass flux through the moving control volume surface, defined by equation (7)

$\dot{q}_m$  = metabolic heat generation rate

$s$  = frozen-unfrozen interface location

$t$  = time

$t_0$  = time of formation of the first ice crystals

$T$  = temperature

$T_a$  = arterial systemic blood temperature

$T_0$  = initial temperature

$T_{ph}$  = phase change temperature

$\dot{w}_b$  = blood perfusion rate

$x$  = length

$x_0$  = characteristic length

$\bar{x}$  = length inside control volume, defined in Fig. 1

$\alpha$  = thermal diffusivity

$\beta$  =  $\dot{w}_b c_b x_0^2 / k$ , nondimensional blood perfusion flow rate

$\gamma$  =  $\dot{w}_b c_b / k$

$\rho$  = density

$\epsilon$  = maximum initial temperature deviation, defined by equation (21)

$\tau$  = Fourier number, defined by equation (19)

$\xi$  =  $x/x_0$ , nondimensional length

### Subscripts

$f$  = frozen tissue

$b$  = blood

by the dashed line at a distance  $s$  from the coordinate origin (i.e., probe surface). Also shown are the heat flux vector,  $\dot{q}$ , and the imaginary mass flux,  $\dot{m}$ , which is discussed in the following.

Solution to the second time domain is obtained in stages. First a solution is sought for the unfrozen region adjacent to the frozen one, i.e.,  $t > t_0$  and  $x > s$ . Mathematically, the problem is stated as follows:

$$\frac{\partial T}{\partial t} = \alpha \frac{\partial^2 T}{\partial x^2} + \frac{\dot{w}_b c_b}{\rho \cdot c_p} (T_a - T) + \frac{\dot{q}_m}{\rho \cdot c_p} \quad (1)$$

with the boundary conditions:

$$T(s, t) = T_{ph} \quad (2)$$

$$T(\infty, t) = T_0 \quad (3)$$

and the initial condition

$$T(x, t_0) = T_0 + (T_{ph} - T_0) \exp \left[ -\frac{\dot{m} c_p}{k} x \right] \quad (4)$$

where  $T_0$  is defined by [9]

$$T_0 = T_a + \frac{\dot{q}_m}{\dot{w}_b c_b} \quad (5)$$

The control volume surface is assumed to move with the frozen-unfrozen tissue interface. A solution was sought so that the resulting cooling rate at the interface be constant and predictable, which is the physiological requirement for controlling tissue destruction rate.

The temperature profile inside the control volume is obtained by writing a quasi-steady heat balance and integrating twice over the region  $\bar{x} = 0$  to infinity. At  $\bar{x} \rightarrow \infty$  an additional adiabatic condition is imposed to yield

$$T = T_0 + (T_{ph} - T_0) \exp \left[ -\frac{\dot{m} c_p}{k} (x - s) \right] \quad (6)$$

which satisfies conditions (2)–(4). Equation (1) is satisfied by equation (6) when  $\dot{m}$  is given by<sup>2</sup>

$$\dot{m} = \frac{\{A + [A^2 + 4\gamma\alpha^2]^{1/2}\} \cdot \rho}{2} \quad (7)$$

and by imposing a constant velocity,  $A$ , of the freezing front

$$\frac{ds}{dt} = A \text{ with } s(t_0) = 0 \quad (8)$$

<sup>2</sup>  $\dot{m}$  is an imaginary mass flux which includes the blood perfusion into and the amount of tissue mass passing through the moving control volume surface.

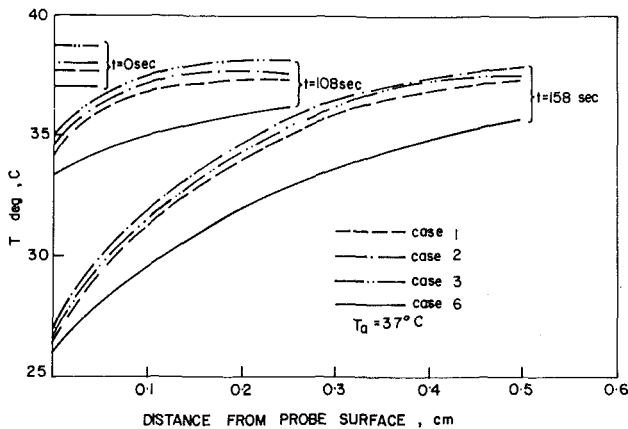


Fig. 2(a) Approximate temperature distributions in the unfrozen tissue as calculated from equation (6) for different cases

For a constant cooling rate,  $\partial T/\partial t(s, t) = H$ , the following expression is obtained

$$A = \left\{ \frac{\alpha^2 \cdot H^2}{\gamma \cdot \alpha^2 (T_{ph} - T_0)^2 + \alpha \cdot H (T_{ph} - T_0)} \right\}^{1/2} \quad (9)$$

Next, the analysis is performed for the frozen region subject to the following equations [18]

$$\frac{\partial T_f}{\partial t} = \alpha_f \frac{\partial^2 T_f}{\partial x^2} \quad t > t_0 \text{ and } x < s \quad (10)$$

$$T_f(s, t) = T_{ph} \text{ with } s = A(t - t_0) \quad (11)$$

$$k_f \frac{\partial T_f}{\partial x}(s, t) = k \frac{\partial T}{\partial x}(s, t) + \rho \cdot L \frac{ds}{dt} \quad (12)$$

Solution to equations (10)–(12) is given by

$$T_f = T_{ph} + B \left\{ 1 - \exp \left[ \frac{A}{\alpha_f} (s - x) \right] \right\} \quad (13)$$

where

$$B = \left\{ \frac{\rho \cdot c_p (T_0 - T_{ph})}{2} \cdot [A + [A^2 + 4\gamma\alpha^2]^{1/2}] + \rho \cdot L \cdot A \right\} \frac{1}{\rho_f c_{pf} A} \quad (14)$$

In the first time domain,  $t < t_0$ , an exact solution to the problem might be obtained by assuming a constant cooling rate at the probe-tissue interface, i.e.,

$$\frac{\partial T}{\partial t}(0, t) = H \quad (15)$$

The governing equation and the additional boundary condition are given by equations (1) and (3), respectively, and the initial condition is given by:

$$T(x, 0) = T_0 \quad (16)$$

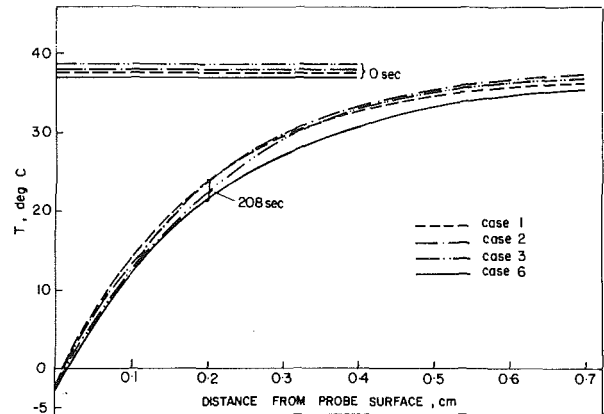


Fig. 2(b) Approximate temperature distributions at the onset of freezing for different cases

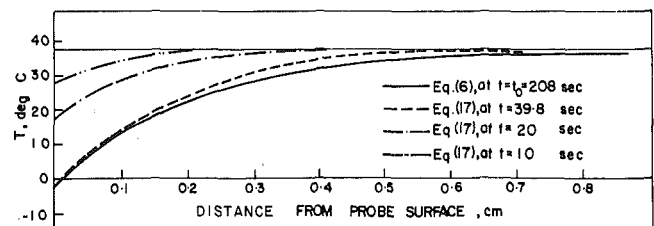


Fig. 2(c) Exact temperature distributions in the unfrozen tissue for case 2 and comparison with the required distribution at the onset of freezing

The solution is obtained by a Laplace transform and is given by

$$T = T_0 + \frac{(T_a - T_0)}{2} \cdot h \left\{ \left( \tau - \frac{\xi}{2\sqrt{\beta}} \right) \exp(-\xi\sqrt{\beta}) \operatorname{erfc} \left( \frac{\xi}{2\sqrt{\tau}} - \sqrt{\beta \cdot \tau} \right) + \left( \tau + \frac{\xi}{2\sqrt{\beta}} \right) \exp(\xi\sqrt{\beta}) \operatorname{erfc} \left( \frac{\xi}{2\sqrt{\tau}} + \sqrt{\beta \cdot \tau} \right) \right\} \quad (17)$$

where

$$h = \frac{H \cdot \rho \cdot c_p \cdot x_0^2}{(T_a - T_0) \cdot k} \quad (18)$$

$$\tau = \frac{tk}{\rho c_p x_0^2} \quad (19)$$

and

$$\xi = \frac{x}{x_0} \quad (20)$$

It turned out that the required initial condition at  $t = t_0$ , i.e., equation (4), could not be satisfied exactly. A maximum deviation of about 7 percent between the desired equation (4), and obtained equation (17), was obtained (see Fig. 2(c)). Thus, a slightly different approach was adopted. Accordingly, it was assumed that the shape of the temperature distribution in the tissue at  $t = t_0$  be identical to the one given by equation (4). This assumption dictates that the temperature profile at  $t < t_0$  and  $x > 0$  be given by equations (6)–(9). However, when equation (6) is examined, it is observed that  $t_0$  should attain a very large value if the initial condition, equation (16), is to be satisfied. This result is due to the exponential nature of equation (6). Thus, an engineering compromise in the form of permitting a slight deviation in the initial condition was required. If  $\epsilon$  denotes this maximum deviation

$$\epsilon \equiv \frac{T(0, 0) - T_0}{T_{ph} - T_0} \quad (21)$$

then  $t_0$  is determined by

$$t_0 = -\frac{k}{m c_p A} \ln \epsilon \quad (22)$$

For the set of physical parameters as given in Table 1,  $t_0$  was calculated at about 39 s. On the other hand, taking  $\epsilon = 0.005$ ,  $t_0$  is obtained at 208 s which is considerably longer; for  $t_0$  to be equal to 39 s the deviation is calculated at about 0.38 which is a prohibitively high value.

## Discussion

First, the effects of the various parameters are examined. From equation (9), with  $T_0$  replaced by equation (5), it is obtained that the velocity of the freezing front,  $A$ , decreases somewhat with increasing the volumetric metabolic rate,  $\dot{q}_m$ . Increasing blood perfusion rate,  $\dot{w}_b$ , also decreases  $A$  but more sharply indicating the importance of this factor in energy transport in the tissue. It follows from equations (4), (5), (7), and (9) that the temperature gradient at the freezing front becomes larger when both  $\dot{q}_m$  and  $\dot{w}_b$  increase. It is also evident, from equation (7), that the effect of  $\dot{w}_b$  is much stronger than that of  $\dot{q}_m$ .

Analysis of the results is performed for the numerical values and 6 cases as given in Tables 1(a) and 1(b). In this table the corresponding values for  $T_0$  as calculated by equation (5) are also shown. Case 6 in which both  $\dot{q}_m$  and  $\dot{w}_b$  vanish is included for completeness and is probably applicable to situations where in vitro freezing occurs. In all cases  $t_0 = 208$  s, such that  $\epsilon < 0.005$ .

Temperature distributions in the unfrozen region, equation (6), when  $t < t_0$ , for cases 1–3 and 6, are shown in Figs. 2(a) and 2(b). It is seen that deviation from the initial temperature remains small for relatively long times and then increases exponentially with time. In Fig. 2(c) the exact solution, equation (17), is plotted for case 2. At  $t = t_0$  both the exact solution and the required one, equation (4), are compared. The maximum deviation found for these two graphs is about 7 percent.

In Fig. 3, temperature distribution in both the frozen and unfrozen regions at  $t = t_0 + 100$  s are shown for all six cases. It is seen that the higher  $\dot{w}_b$  and  $\dot{q}_m$  the closer the location of the frozen front, at  $x = s$ , to the tissue-probe interface. Also, the effects of  $\dot{q}_m$  are seen to be smaller than those of  $\dot{w}_b$ . For the limiting case 6, i.e.,  $\dot{w}_b = \dot{q}_m = 0$ , the tissue-probe interfacial temperature is the lowest at about  $-152^\circ\text{C}$ , increasing to about  $-107^\circ\text{C}$  for case 1.

Probe-tissue interfacial temperature and heat flux and location of the frozen front as functions of time are shown in Figs. 4 and 5. Fig. 4 gives the values for cases 1–3 and 6 whereas Fig. 5 is for cases 2–6 excluding 3. These figures again support the previous observations regarding the freezing front velocity and the probe-tissue interface temperature. It is observed in Fig. 5 that the effect of varying  $\dot{q}_m$  on the temperature distribution in the tissue is very small and might be neglected without introducing large errors. It is also seen that the heat flux is larger for smaller values of  $\dot{w}_b$  and  $\dot{q}_m$ . Another result is associated with a limited minimal probe temperature which might be due to the use of different cryofluids. When this limitation is considered coincidental with the desired constant cooling rate, it is obtained that the higher  $\dot{w}_b$  and  $\dot{q}_m$ , the deeper the extent of destruction of the tissue.

Table 1 Physical and thermophysical properties

$c_p$ , $\frac{\text{kJ}}{\text{kg}^\circ\text{C}}$	$c_b$ , $\frac{\text{kJ}}{\text{kg}^\circ\text{C}}$	$k$ , $\frac{\text{W}}{\text{m}^\circ\text{C}}$	$k_f$ , $\frac{\text{W}}{\text{m}^\circ\text{C}}$	$\alpha$ , $\frac{\text{m}^2}{\text{s}}$	$\alpha_f$ , $\frac{\text{m}^2}{\text{s}}$	$L$ , $\frac{\text{kJ}}{\text{kg}}$	$H$ , $\frac{^\circ\text{C}}{\text{s}}$	$T_{ph}$ , $^\circ\text{C}$
3.72	3.64	0.46	1.4	11	33	285	-1	-2

(a)

Case	1	2	3	4	5	6
$\dot{q}_m$ , $\frac{\text{kW}}{\text{m}^3}$	251	251	251	167	84	0
$\dot{w}_b$ , $\frac{\text{kg}}{\text{m}^3\text{s}}$	10	7.0	4.0	7.0	7.0	0
$T_0$ , $^\circ\text{C}$	37.7	38	38.7	37.6	37.3	37

(b)

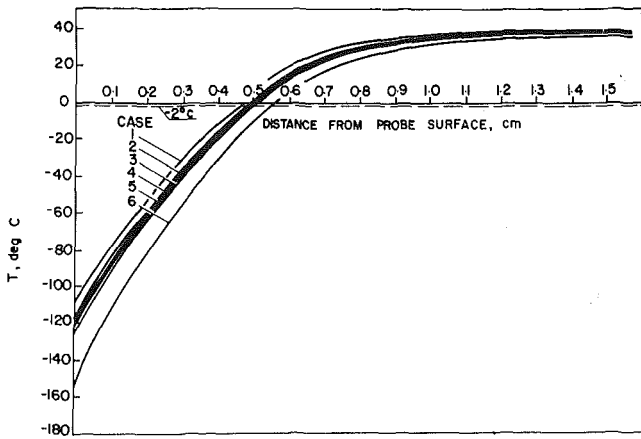


Fig. 3 Temperature distributions in both the frozen and unfrozen regions 100 s after freezing commenced for all six cases

Fig. 6 shows typical temperature distributions for case 2. For the assumed set of parameters and a minimum probe temperature of  $-180^{\circ}\text{C}$  the depth of freezing is 6.4 mm reached 133 s after formation of the first ice crystals. This result is also easily obtained from Figs. 4 and 5.

Results of the present work were compared to those reported previously. It is found that Warren and co-workers obtained the same slowing effect of blood perfusion on the velocity of the freezing front [11]. When examining their cooling rates at the frozen front, they found a  $-7^{\circ}\text{C}/\text{s}$  temperature drop for  $s = 0$  decreasing to  $-1^{\circ}\text{C}/\text{s}$  at a depth of 6 mm reached 120 s after initiation of freezing. These results were obtained for a minimum probe temperature of  $-160^{\circ}\text{C}$ . These cooling rates could be inside the range where a considerable number of cells may survive freezing, depending on the tissue type [1]. In the present work, with heat capacity and heat generation considered, and for a constant cooling rate of  $-1^{\circ}\text{C}/\text{s}$ , the frozen front is located at a depth of about 6.1 mm after 120 s (see Fig. 4). Trezek and Cooper obtained similar results for spherical coordinates [9].

## Conclusions

An analysis of a Stefan-like problem in the freezing of a biological tissue in cartesian coordinates is presented. Blood perfusion and metabolic heat generation rates are included in the thermal energy balance of the tissue. Heat capacity of the tissue is also considered and the solution is obtained for a constant imposed cooling

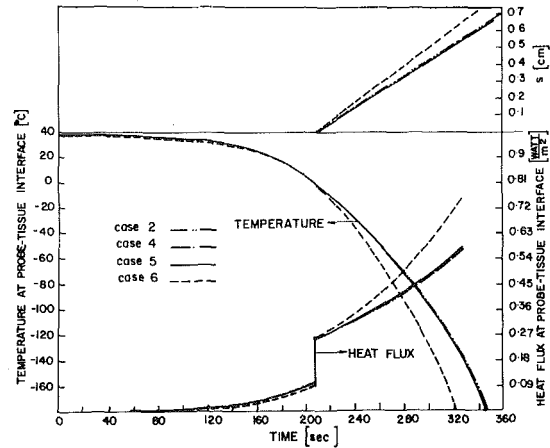


Fig. 5 Probe temperature and heat flux variations and location of the frozen front for various metabolic heat rates

rate at the freezing front.

Based on this analysis, the following conclusions are drawn:

1 The effect of metabolic heat generation rate,  $\dot{q}_m$ , on the temperature distribution in the tissue is small and might, therefore, be neglected without causing significant errors in the results. On the other hand, blood perfusion effects are significant both in regard to the location of the freezing front and the temperature distribution in the tissue.

2 The occurrence of small values of blood perfusion and metabolic rate cause a high velocity of the freezing front with a small depth of the frozen region.

Results presented in this work facilitate the estimation of required probe temperature and heat flux variations such that a constant cooling rate at the freezing front is achieved. As indicated previously, the present cartesian model yields values close to those obtained by the spherical or cylindrical models. These results allow, therefore, the surgeon to employ a controlled cryoprocess for optimal results in tissue destruction.

## References

- 1 Farrant, J., "Cryobiology—The Basis to Cryosurgery," in *Cryogenics in Surgery*, Medical Examination Publishing Co. Inc., June 1971.
- 2 Meryman, H. T., "Mechanics of Freezing in Living Cells and Tissues," *Science*, Vol. 124, Sept. 1956, pp. 515–521.
- 3 Leibo, S. P., and Mazur, P., "The Role of Cooling Rates in Low Temperature Preservation," *Cryobiology*, Vol. 8, 1971, pp. 447–452.
- 4 Ling, G. R., and Tien, C. L., "An Analysis of Cell Freezing and Dehydration," *JOURNAL OF HEAT TRANSFER, TRANS. ASME, Series C*,

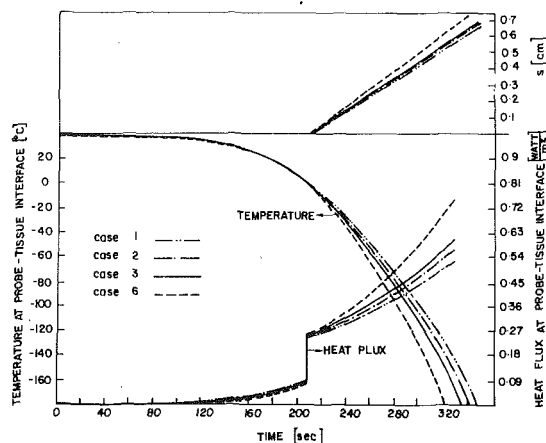


Fig. 4 Probe temperature and heat flux variations and location of the frozen front for various blood perfusion rates

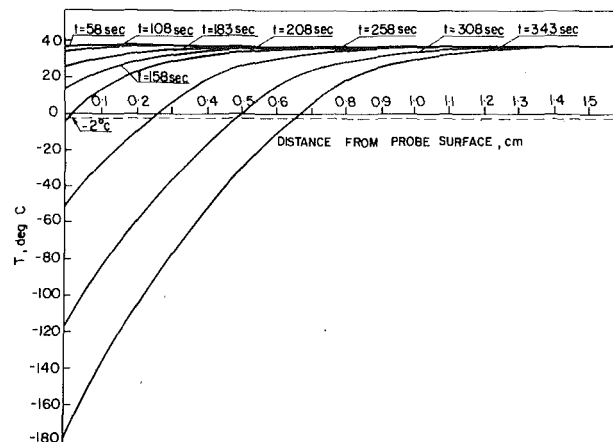


Fig. 6 Temperature distributions in both the frozen and unfrozen regions for case 2

Vol. 92, No. 3, 1970, pp. 393-397.

5 Diller, K. R., "Intracellular Freezing: Effect of Extracellular Supercooling," *Cryobiology*, Vol. 12, Oct. 1975, pp. 480-485.

6 Toscano, W. M., Cravalho, E. G., Silveras, O. M., and Huggins, C. E., "The Thermodynamics of Intracellular Ice Nucleation in the Freezing of Erythrocytes," *JOURNAL OF HEAT TRANSFER, TRANS. ASME, Series C*, Vol. 97, 1975, pp. 326-332.

7 Barron, R. F., "Cryoinstrumentation," in *Cryogenics in Surgery*, Medical Examination Publishing Co. Inc., June 1971.

8 Barron, R. F., "Heat Transfer Problems in Cryosurgery," *J. Cryosurgery*, Vol. 1, 1968, pp. 316-325.

9 Cooper, T. E., and Trezek, G. J., "Mathematical Predictions of Cryogenic Lesion," in *Cryogenics in Surgery*, Medical Examination Publishing Co. Inc., June 1971.

10 Cooper, T. E., and Trezek, G. J., "Rate of Lesion Growth Around Spherical and Cylindrical Cryoprobe," *Cryobiology*, Vol. 7, No. 4, 1971, p. 6.

11 Warren, R. P., Bingham, P. E., and Carpenter, J. D., "Heat Flow in Living Tissue During Cryosurgery," ASME Paper No. 74-WA/Bio-6, 1974.

12 Pennes, H. H., "Analysis of Tissue and Critical Blood Temperatures in the Resting Human Forearm," *J. Appl. Phys.*, Vol. 1, 1968, pp. 93-122.

13 Shitzer, A., and Kleiner, M. K., "Thermal Behaviour of Biological Tissues -- A General Analysis," to appear in *Bulletin of Mathematical Biology*, 1976.

14 Rothenberg, H. W., "Cutaneous Circulation in Rabbits and Humans Before, During, and After Cryosurgical Procedures Measured by Xenon-133 Clearance," *Cryobiology*, Vol. 6, No. 6, 1970, pp. 507-511.

15 Walder, H. A. D., "Experimental Cryosurgery," in *Cryogenics in Surgery*, Medical Examination Publishing Co. Inc., June 1971.

16 Chato, J. C., "A Method for the Measurement of the Thermal Properties of Living Tissue," *Thermal Problems in Biotechnology*, ASME Symposium Series, 1968, pp. 16-25.

17 Freedman, S. J., *Ablation in Developments in Heat Transfer*, London, 1964.

18 Langford, D., "New Analytical Solutions of the One Dimensional Heat Equation for Temperature and Heat Flow Rate Both Prescribed at the Same Fixed Boundary (With Application to the Phase Change Problem)," *Quart. Appl. Math.*, Vol. XXIV, No. 4, 1967, pp. 316-322.